

Intelligent controller based WECS fed unified power flow conditioner for PQ enhancement

Polishetty Vinay Kumar¹, Balamurugan Ganapathi¹, Jayaraman Kartigeyan²

¹Department of Electrical and Electronics Engineering, Annamalai University, Chidambaram, India

²Department of Electrical and Electronics Engineering, J. B. Institute of Engineering and Technology, Hyderabad, India

Article Info

Article history:

Received Feb 25, 2023

Revised Apr 16, 2023

Accepted May 3, 2023

Keywords:

CFLC

DFIG based WECS

DQ theory

Power quality

UPFC

ABSTRACT

The dominance of non-linear loads, sustainable energy sources and power electronic devices in modern power system has in turn compromised the system stability by introducing numerous power quality (PQ) issues. A wind energy conversion system (WECS) fed unified power flow conditioner (UPFC) architecture is suggested in this work since maintaining optimal PQ is important for both the supply authorities and customers. The proposed approach supports both clean energy generation and PQ enhancement. The UPFC aids with accomplishing control over reactive power flow, active power flow, phase angle, impedance and voltage. The reference current for the UPFC is generated using DQ theory. Moreover, a shunt and series compensators of an UPFC are controlled using cascaded fuzzy logic controller (CFLC). The stability of the DC voltage obtained from doubly fed induction generator (DFIG) based WECS is also controlled using a CFLC. The simulation model for the presented WECS fed UPFC is developed in MATLAB and its performance is evaluated.

This is an open access article under the [CC BY-SA](https://creativecommons.org/licenses/by-sa/4.0/) license.



Corresponding Author:

Polishetty Vinay Kumar

Department of Electrical and Electronics Engineering, Annamalai University

Annamalai Nagar, Chidambaram, Tamil Nadu 608002, India

Email: vinaykumarpolishetty@gmail.com

1. INTRODUCTION

Electrical energy is regarded a vital component that ensures socioeconomic development. However, the intensifying threat of climate change and rapidly depleting fossil fuels, has in turn prompted the factors such as environment and resources to become major constraints affecting electrical energy generation. Consequently, the world is currently confronted with serious issues such as sustainable energy production, energy resource conservation, and environmental security. Moreover, the factors such as industrialization, urbanization and population growth has resulted in the continuous increase in demand for electrical energy. Thereby, the development and expansion of sustainable energy is the only solution to resolve all these crisis [1]–[3]. Over the past two decades, the sustainable energy source of wind energy has witnessed exponential growth with an overall installed capacity exceeding 733 GW in the year 2021 [4]. On the flip side, the expansion of wind power generation worsens a stable operation of the power networks with an emergence of several PQ issues. The fundamental reason for this is that a WECS is stochastic and intermittent [5]. Moreover, the large-scale infusion of wind farms and other sustainable energy sources requires the extensive use of power electronic devices, which in turn has complicated the architecture of the power network. The increase in number of nonlinear loads has also resulted in an onset of several PQ issues, leading to stability imbalance in the power system [6]. Thereby, the improvement of power system reliability by minimizing PQ issues has to be prioritized simultaneously with increasing the sustainable energy [7]. The usage of flexible

alternating current transmission systems (FACTS) devices is one of the efficient current methods for reducing the negative effects of PQ concerns.

A FACTS device modifies power system parameters such as bus voltage, reactive and active power flow, and line impedance in order to enhance an electric system's capacity for transferring power, stability, and controllability [8]. FACTS devices are generally divided into two generations. The first generation of FACTS components includes the static VAR compensator (SVC), thyristor-controlled series capacitor (TCSC), and thyristor-controlled phase shifting transformer. These devices are primarily based on an idea of thyristor switched reactors and capacitors. Devices from the second generation of FACTS include the static synchronous series compensator (SSSC), static synchronous compensator (STATCOM), interline power flow controller, and upstream power compensator. These devices are based on the idea of gate turn off thyristor switched converters. The SVC [9] minimizes the system losses by compensating PQ issues and enhancing the transient stability. The TCSC [10] improves a dynamic and transient stability of a system in addition to enriching its power flow. The STATCOM [11] is effective in minimizing the current harmonics and provides a comparatively better damping characteristics than SVC. Second generation FACTS devices are considered to be a more appropriate choice in many practical applications. The current harmonics effectuated by non-linear loads are minimized effectively with the application shunt active filter [12]. However, its performance is affected by the impact of supply voltage. The fluctuations in system voltage are compensated by using dynamic voltage restorer (DVR) [13] but it is inept in minimizing higher level voltage sags. Moreover, all these aforementioned techniques are designed only to solve a specific type of PQ issue. Thereby, a UPFC [14]–[16] is considered for curtailing PQ issues in this work. This versatile FACTS device, which entails both shunt and series compensators in its design, ensures power control along with enhancement of the transient stability. The direct-quadrature (DQ) theory is used for generation of reference current for an UPFC in this work.

The choice of an efficient controller is vital for controlling the working of the UPFC. One of the most widely used controller application is PI controller [17], which improves the system performance by regulating the DC quantities with its simple topology. However, it is incapable of handling non-linear and dynamic operating conditions, resulting in non-zero steady state error. Consequently, techniques such as FLC [18] and artificial neural network (ANN) [19], which comes under artificial intelligence-based control approaches are employed. The FLC is suitable for tackling non-linear operating conditions with high accuracy. Its processing speed is inversely proportional to the number of rules used, thus the FLC provides delayed dynamic response with the increase in number of rules. The ANN is characterized with quick processing speed but it is not capable of providing highly accurate outcomes. Thereby a CFLC controller, which offers accurate output within quick processing time is proposed as a suitable controller approach in this work.

A WECS fed UPFC design with appropriate control approaches is proposed in this work for promoting decarbonized sustainable energy production along with curbing PQ disturbances. Here, CFLC is used for stabilizing the WECS output by controlling the PWM rectifier interfaced to the DFIG based WECS. Moreover, a series and shunt compensators of an UPFC are also regulated with the assistance of CFLC. The proposed approach is validated to ascertain its effectiveness using MATLAB simulations.

2. RELATED WORKS

An UPFC is developed which adopts a model-free adaptive control approach for improving the functioning of the WECS as explained in [20]. The proposed work facilitates the effective working in conditions of wind gusts along with the enhancement of fault ride through capability. The obtained outputs indicate the simple implementation, rapid response, robustness and adaptive nature. In spite of these merits, issues related to overshoot occurs in this work.

An optimal reactive power dispatch approach is proposed to deliver power to grid along with ACO algorithm with ANFIS controller as show in [21]. By allowing for the power sharing between AC zones, the suggested control technique can regulate the frequency to desired level even when there is little wind power available. Unfortunately, due to compensating methods and unpredictable nature of control operation, there occurs specialist challenges.

Sankarganesh *et al.* [22] introduced UPFC, a novel hybrid device, manages the flow of DC voltage in the electrical power transmission network. The proposed reference voltage-current estimator's structure allows for the simultaneous adjustment of reactive power at the basic grid frequency, voltage harmonics, and current harmonics while minimizing voltage dips and overvoltage. Despite of its merits, oscillation damping of power occurs.

An evaluation framework was developed to address power quality challenges that have emerged following an integration of substantial wind farms into inadequate transmission systems as described in [23]. The challenges like voltage profiles, stability, voltage and current harmonics, and power fluctuations at PCC, which take seasonal variations and heavy loading situations are helped by this research. The work becomes inappropriate if the main concern is towards power quality issue.

The results in [24], a system control design for marine motion control susceptible to hostile environments was presented. This offers a potent and responsive tool for creating reliable control systems that operate in challenging conditions. Poor state assessment will happen if harsh disruptions and unmodeled dynamics are not taken into account, which would then lead to decreased control precision.

The word in [25], LMI technique is utilized to enhance a dynamic stability of power system with UPFC and DFIG. A small portion of the total power is provided by power electronic converters. As a result, losses in power electronic converter are decreased, and system cost is lower because the power electronics are only partially rated. The search techniques could also get stuck in a local minimum, and the result might not be the best.

3. PROPOSED SYSTEM DESCRIPTION

The environmental and resource constraints that affect fossil fuel-based energy generation has resulted in the shifting of focus towards sustainable energy sources for satisfying the ever-increasing energy demand. Thereby, the generation of power using wind energy is witnessing tremendous growth in recent times. However, the intermittent nature of wind energy compromises a stability of the power system with an onset of PQ issues. Hence, a WECS fed UPFC design is proposed in this work as seen in Figure 1, to curb PQ disturbances and improve the stability of WECS integrated power system.

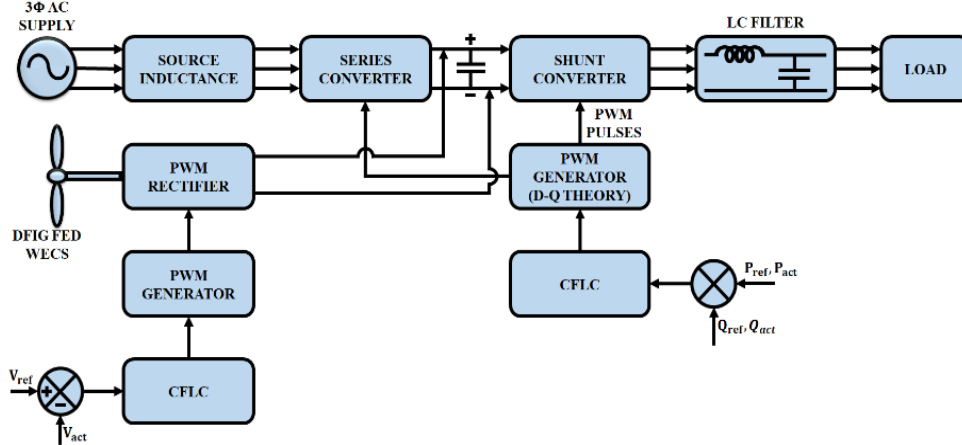


Figure 1. Structure of the proposed WECS fed UPFC

The proposed work considers a DFIG based WECS owing to its adaptability, efficiency and flexibility. The DC output obtained from the PWM rectifier, which is interfaced to the DFIG based WECS is provided to DC-link of the UPFC. A shunt and series converters of an UPFC are also connected to DC-link. Moreover, coupling transformers are used to connect these two converters to the power system. The UPFC enhances the PQ of the system by controlling the phase angle, impedance, voltage, reactive and real power flow. PWM rectifier is controlled using CFLC, which aids with obtaining a stable distortion free output from the WECS. The reference current for the UPFC is generated using DQ theory, while CFLC is used for controlling an operation of the UPFC converters.

4. PROPOSED SYSTEM MODELLING

4.1. Modelling of UPFC

The UPFC design comprises of two converters connected back-to-back through a common DC-link as illustrated in Figure 2(a). Here, one voltage source converter (VSC) is shunt connected to the bus (i), while another VSC is series connected to the transmission line. In this work, the output from DFIG based WECS is also connected to a common DC-link. Both a series and shunt compensators are interfaced to the system via a series and shunt coupling transformers (T_{se} and T_{sh}) respectively. Figure 2(b) presents an equivalent circuit of UPFC. Shunt impedance and series impedance are represented using the terms Z_{sh} and Z_{se} respectively. The power flow problem is solved by using the following NR matrix as (1)-(4).

$$[J][X] = [B] \tag{1}$$

$$[B] = \begin{bmatrix} \Delta P \\ \Delta Q \end{bmatrix} \tag{2}$$

$$[J] = \begin{bmatrix} J_{P\delta} & J_{PV} \\ J_{Q\delta} & J_{QV} \end{bmatrix} \tag{3}$$

$$[X] = \begin{bmatrix} \Delta\delta \\ \Delta V/V \end{bmatrix} \tag{4}$$

Where, the phase angle and voltage magnitude vector are specified as X , the Jacobian matrix is specified as J , the power mismatch of the reactive and active powers are specified as B and the Jacobian matrix elements are represented as $J_{P\delta}, J_{PV}, J_{QV}$ and $J_{Q\delta}$.

$$(J_{P\delta})_{ij} = \frac{\partial P_i}{\partial \delta_j} \tag{5}$$

$$(J_{PV})_{ij} = \frac{\partial P_i}{\partial V_j} V_j \tag{6}$$

$$(J_{Q\delta})_{ij} = \frac{\partial Q_i}{\partial \delta_j} \tag{7}$$

$$(J_{QV})_{ij} = \frac{\partial Q_i}{\partial V_j} V_j \tag{8}$$

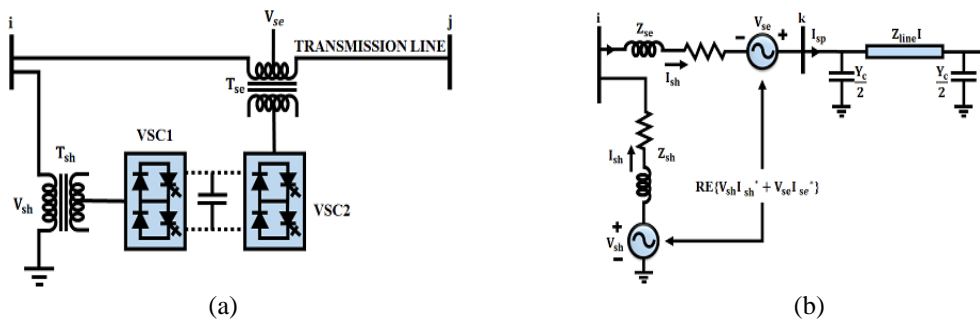


Figure 2. UPFC: (a) schematic diagram and (b) equivalent circuit

4.1.1. Modelling of series converter

In a transmission line, a reactive and active power flow is controlled using a series compensator by injecting series voltage of controllable phase angle and magnitude. As illustrated in Figure 3(a), a series converter is modelled as a current source (I_{inj}) shunt connected to its impedance by converting a series voltage source (V_{se}) on the basis of (9). For representing the UPFC terminals, an auxiliary bus is added and the power flow direction is realized. Figure 3(b) represents current source as shunt injected current.

$$I_{inj} = \frac{V_{se}}{Z_{se}} \tag{9}$$

$$I_{inj} = I_{kj} - I_{ik} = \left(\frac{S_{sp}}{V_k}\right) - \left(\frac{V_i - V_k}{Z_{se}}\right) \tag{10}$$

Here,

$$S_{sp} = P_{sp} + jQ_{sp} \tag{11}$$

$$I_{kj} = I_{sc} = \left(\frac{S_{sp}}{V_k}\right)^* \tag{12}$$

The representation of shunt injected current as complex loads is illustrated in Figure 4. The loads are updated as follows during load flow iterative process as (13) and (14).

$$S_i = V_i(I_{inj})^* \tag{13}$$

$$S_k = -V_k(I_{inj})^* \tag{14}$$

An active power injected by a series compensator is given as (15).

$$P_{ex1} = P_{se} = Re(V_{se}(I_{se})^*) \tag{15}$$

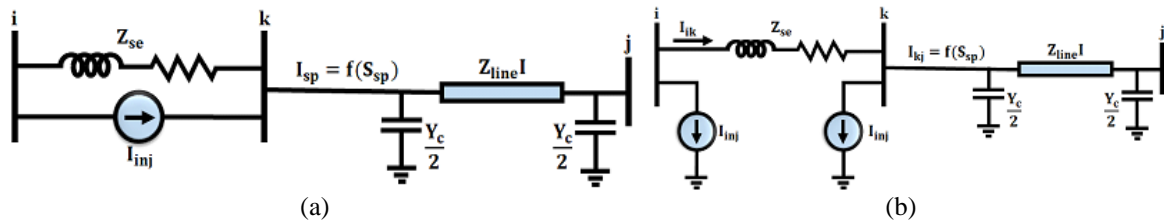


Figure 3. Representation of UPFC series converter on the basis of (a) current source and (b) injected current

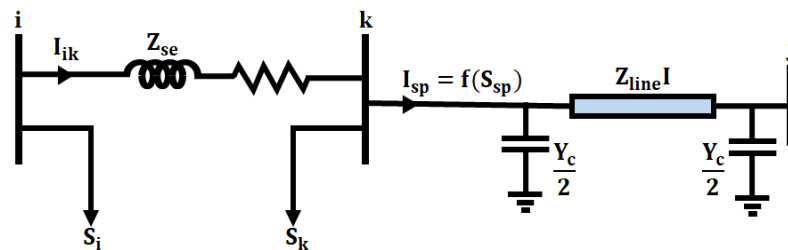


Figure 4. Representation of UPFC on the basis of injected loads

4.1.2. Modelling of shunt converter

The bus voltage is controlled through injection or absorption of reactive power by the shunt converter. A shunt injected power is expressed as (16) and (17).

$$P_{ex2} = P_{sh} = Re(V_{sh}(I_{sh})^*) \tag{16}$$

$$P_{sh} + P_{se} = 0 \tag{17}$$

The injected reactive power is represented as (18).

$$Q_{sh} = \sum_{i=1}^n V_i V_n (G_{in} \sin \delta_{in} - B_{in} \cos \delta_{in}) + Q_i^{load} + Q_i \tag{18}$$

The equivalent circuit of shunt converter is illustrated in Figure 5(a) and Figure 5(b) represents the circuit when load is applied and condenser configuration in seen in Figure 5(c). The shunt current and shunt voltage is expressed as (19) and (20).

$$V_{sh} = V_i + Z_{sh} \left(\frac{P_{sh} + jQ_{sh}}{V_i} \right)^* \tag{19}$$

$$I_{sh} = \frac{V_{sh} - V_i}{Z_{sh}} = \left(\frac{P_{sh} + jQ_{sh}}{V_i} \right) \tag{20}$$

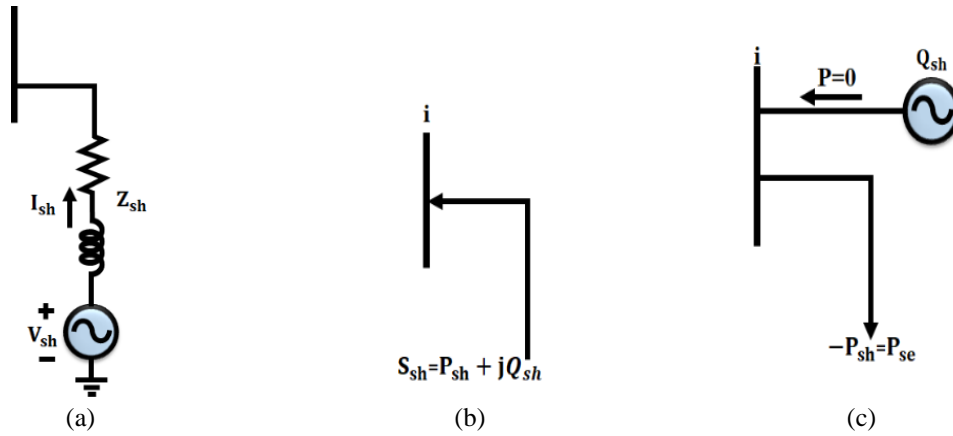


Figure 5. Representation of UPFC shunt converter: (a) equivalent circuit, (b) load injection, and (c) condenser

4.2. CFLC and DQ theory-based control of UPFC

The power components are measured with the application of DQ theory. This time-domain based approach is relevant for both transient and steady state systems and is applied on generic waveforms of voltage and current. Moreover, its computational simplicity is also regarded as its major advantage. It mainly comprises of algebraic calculations aside from those needed to separate mean and alternated values of power component estimation. The park transformation is used for obtaining d-q coordinates (rotating coordinates) by transforming a-b-c coordinates.

$$\begin{bmatrix} v_d \\ v_q \\ v_0 \end{bmatrix} = \frac{2}{3} \begin{bmatrix} \cos(\phi) & \cos(\phi - \frac{2\pi}{3}) & \cos(\phi + \frac{2\pi}{3}) \\ -\sin(\phi) & -\sin(\phi - \frac{2\pi}{3}) & -\sin(\phi + \frac{2\pi}{3}) \\ \frac{1}{2} & \frac{1}{2} & \frac{1}{2} \end{bmatrix} \begin{bmatrix} v_a \\ v_b \\ v_c \end{bmatrix} \tag{21}$$

$$\begin{bmatrix} i_d \\ i_q \\ i_0 \end{bmatrix} = \frac{2}{3} \begin{bmatrix} \cos(\phi) & \cos(\phi - \frac{2\pi}{3}) & \cos(\phi + \frac{2\pi}{3}) \\ -\sin(\phi) & -\sin(\phi - \frac{2\pi}{3}) & -\sin(\phi + \frac{2\pi}{3}) \\ \frac{1}{2} & \frac{1}{2} & \frac{1}{2} \end{bmatrix} \begin{bmatrix} i_a \\ i_b \\ i_c \end{bmatrix} \tag{22}$$

$$\phi = (\omega t + \theta) \tag{23}$$

Where, the phase shift between the fixed and rotating coordinates is specified as ϕ , while a phase shift between a line current and voltage is specified as θ . The active and reactive power components are estimated as (24) and (25).

$$p = V_d I_d + V_q I_q \tag{24}$$

$$q = V_d I_q - V_q I_d \tag{25}$$

4.2.1. CFLC based compensator control scheme

The compensator control scheme for UPFC using DQ theory and CFLC is illustrated in Figure 6. The measured currents and voltages are initially low pass filtered to remove high frequency noise components. Subsequently, power components (reactive and active) are estimated using park transformation and given as input to the CFLC. The modulation index for the PWM generator, which controls the operation of the compensators is obtained as output from the CFLC.

The CFLC approach used in this work is the cascaded connection of two FLC controllers. Moreover, the CFLC is provided with four inputs and has five membership functions. The normal FLC controller with four inputs and 5 membership functions require $5^4 = 625$ rules, while CFLC requires just 50 rules ($5^2 + 5^2$). Thus, the computational time is significantly reduced in case of CFLC approach, resulting in quicker response.

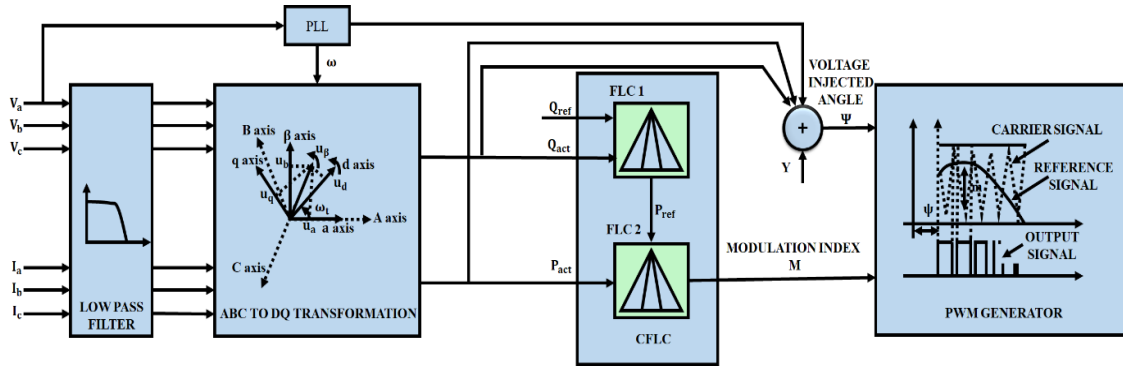


Figure 6. Structure of CFLC and DQ theory-based compensator control

4.3. Modelling of DFIG based WECS

The WECS is a variable power source unlike the conventional power generation systems. Here, the DFIG is used as the generator technology for WECS due to its excellent efficiency and adaptability. The structure of the DFIG based WECS is given in Figure 7.

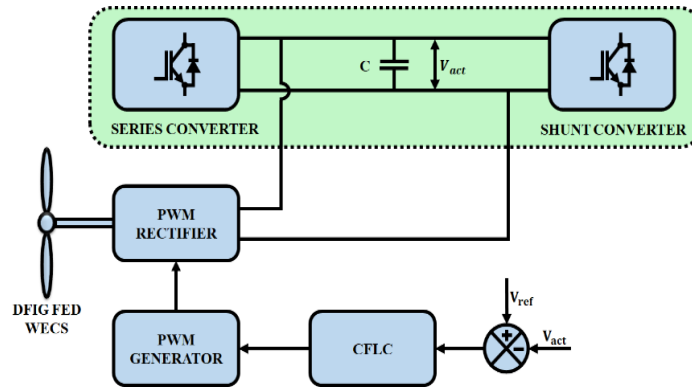


Figure 7. Structure of WECS fed UPFC

4.3.1. Wind speed model

A wind speed frequency distribution is characterized using Weibull probability distribution. The c-scale parameter (m/s) and k-form parameter (dimensionless) constitutes this distribution model. The expression for Weibull distribution is given as (26).

$$f_v(v) = \frac{k}{c} \left(\frac{v}{c}\right)^{k-1} \left[-\left(\frac{v}{c}\right)^k\right] \tag{26}$$

Where, the speed and occurrence frequency of wind are specified as v and $f_v(v)$ respectively.

4.3.2. Turbine model

The DFIG generates electrical energy by converting the mechanical energy produced by the turbine blades. The turbine mechanical power obtained from wind is expressed as (27).

$$P_m = C_p(\lambda, \beta) \frac{\rho A}{2} V_\omega^3 \tag{27}$$

Where, the terms β , λ , V_ω , A and ρ represents the blade inclination angle, speed ratio, wind speed, turbine swept area and air density respectively. The power coefficient is denoted as (28).

$$C_p(\lambda, \beta) = 0.5176 \left(\frac{116}{\lambda_i} - 0.4\beta - 5\right) e^{-\frac{21}{\lambda_i}} + 0.0068\lambda \tag{28}$$

Where the parameter λ_i is expressed as (29).

$$\frac{1}{\lambda_i} = \frac{1}{\lambda + 0.08\beta} - \frac{0.035}{\beta^3 + 1} \quad (29)$$

4.3.3. DFIG model

The DFIG dynamic modelling in d-q reference frame is expressed as (30).

$$\begin{cases} v_{ds} = R_s i_{qs} + \omega_s \psi_{qs} + \frac{d\psi_{ds}}{dt} \\ v_{qs} = R_s i_{qs} + \omega_s \psi_{ds} + \frac{d\psi_{qs}}{dt} \\ v_{dr} = R_r i_{dr} + (\omega_s - \omega_r) \psi_{qr} + \frac{d\psi_{dr}}{dt} \\ v_{qr} = R_r i_{qr} + (\omega_s - \omega_r) \psi_{dr} + \frac{d\psi_{qr}}{dt} \end{cases} \quad (30)$$

Here,

$$\begin{cases} \psi_{ds} = L_s i_{ds} + L_m i_{dr} \\ \psi_{qs} = L_s i_{qs} + L_m i_{qr} \\ \psi_{dr} = L_r i_{dr} + L_m i_{ds} \\ \psi_{qr} = L_r i_{qr} + L_m i_{qs} \end{cases} \quad (31)$$

In d-q axis, the stator voltages, currents and flux are represented as v_{ds} , v_{qs} , i_{ds} , i_{qs} , ψ_{ds} and ψ_{qs} respectively. Similarly, the rotor voltages, currents and flux are represented as v_{dr} , v_{qr} , i_{dr} , i_{qr} , ψ_{dr} and ψ_{qr} respectively. The resistance and inductance of the rotor and stator are specified as R_r , R_s , L_r and L_s respectively. The magnetising inductance is specified as L_m . The electromagnetic torque is given as (32).

$$T_{em} = \frac{3}{2} p (\psi_{ds} i_{qs} - \psi_{qs} i_{ds}) \quad (32)$$

The active and reactive stator output is given as (33) and (34).

$$P_s = \frac{3}{2} (v_{ds} i_{ds} - v_{qs} i_{qs}) \quad (33)$$

$$Q_s = \frac{3}{2} (v_{qs} i_{ds} - v_{ds} i_{qs}) \quad (34)$$

The active and reactive rotor output is given as (35) and (36).

$$P_r = \frac{3}{2} (v_{dr} i_{dr} - v_{qr} i_{qr}) \quad (35)$$

$$Q_r = \frac{3}{2} (v_{qr} i_{dr} - v_{dr} i_{qr}) \quad (36)$$

Here, the number of poles is represented using the term p . The output from the DFIG is converted to DC voltage using PWM rectifier, while the rectifier is controlled using CFLC based closed loop control.

4.4. CFLC based control for WECS

The CFLC is used for error compensation and it control the switching operation of PWM rectifier interfaced to the WECS. The CFLC is mainly employed in the WECS to stabilize its output and always ensure a constant fluctuation free output from the WECS. As mentioned above, the effectiveness of CFLC in offering quick and accurate dynamic response, accredits to its choice as an appropriate controller. The structure of the CFLC includes two FLCs, which are series connected as seen in Figure 8. The duty ratio range for FLC 2 is narrowed down by FLC 1. The FLC replicates the operation of an expert human operator. It simulates human reasoning to obtain definite solution for problems involving inadequate and imprecise data.

The actual output voltage of the PWM rectifier V_{act} is compared to the reference voltage V_{ref} to estimate the error e . An obtained error and its change rate (ce) are provided as input to the FLC. The fuzzifier of the FLC converts e and ce in to linguistic fuzzy sets. An evaluation of control rules in the rule base and generation of fuzzy sets are subsequently done by an inference engine using fuzzified measures. The final defuzzification block converts the fuzzy set obtained as output in to crisp value. The fuzzy rules are expressed as (37).

$$R_i: \text{If } e \text{ is } A_i, ce \text{ is } B_i \text{ then } \delta m_n \text{ is } C_i \tag{37}$$

Where the fuzzy sets are represented as A_i, B_i and C_i . The standardized values of error and its change rate is $[-1,1]$, while $[-1,1]$ is the range of m, n . A maximum of 25 rules is obtained for every combination of e and ce . The rule base is given in Table 1. The inference engine result is given as (38) and (39).

$$Z_i = \min\{\mu_e(e), \mu_{ce}(ce)\}. C_i \tag{38}$$

$$Z_i = W_i C_i \tag{39}$$

Where, the modulated signal's rate of membership is specified as C_i and the weighting function precise rule is given as W_i .

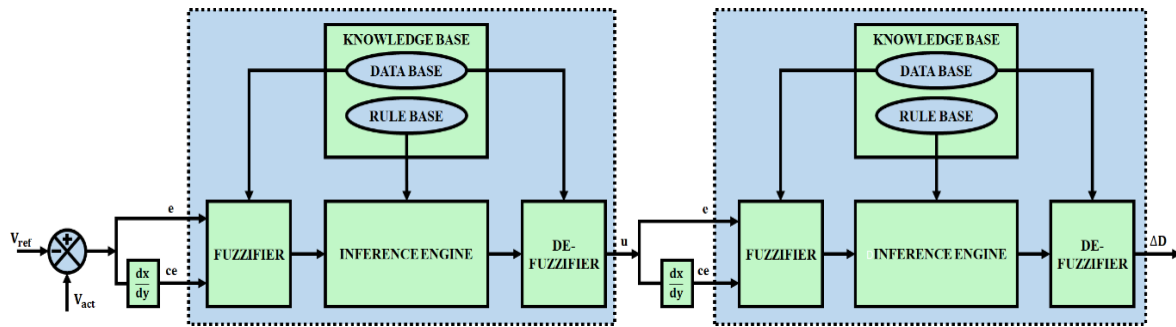


Figure 8. CFLC approach

Table 1. FLC rule base

Fuzzy Rules	e					
	NB	NS	ZE	PS	PB	PB
NB	ZE	ZE	PB	PB	PB	PB
NS	ZE	ZE	PS	PS	PS	PS
ce	ZE	PS	ZE	ZE	ZE	NS
	PS	NS	NS	NS	ZE	ZE
	PB	NB	NB	NB	ZE	ZE

*ZE=Zero, PS=Positive Small, PB=Positive Big, NB=Negative Big and NS=Negative Small

5. RESULTS AND DISCUSSION

A WECS fed UPFC design with novel control approaches that supports both sustainable energy generation and PQ disturbances minimization is proposed in this work. The proposed WECS fed UPFC model is tested for its performance with the aid of MATLAB. Figure 9 represents the simulation setup of the proposed work and Table 2 gives the parameter specifications for the simulation model.

i) Case 1: Step magnitude -0.3

The proposed WECS fed UPFC design is tested for its effectiveness in both voltage sag and voltage swell conditions. Case 1 evaluates the practicability and applicability of the proposed WECS fed UPFC while encountering Voltage sag and the concerned waveforms are given in Figure 10 and Figure 11. Thereby, a 400 V source voltage encounters a 0.3 p.u voltage sag between 0.1s and 0.2s as seen in Figure 10. The input current experiences an increase in magnitude to 50 A during the occurrence of voltage sag. For obtaining a clear understanding about the source voltage and current waveform during case 1, a single phase (phase A) of both these parameters are also considered. On observing the load side waveforms, it is concluded that the proposed WECS fed UPFC design successfully compensates the voltage sag, since both the load voltage and load current waveforms are stable in nature. Moreover, due to the accurate compensation of voltage sag, unity power factor is maintained. Figure 10 also gives the real power and reactive power waveforms. Figure 11 illustrates the reference voltage and current signals in addition to an actual voltage and current signals of an UPFC. The reference signals for the compensators are generated with the assistance of DQ theory and CFLC. It is observed that the compensators generate the necessary voltage for compensating the voltage sag condition.

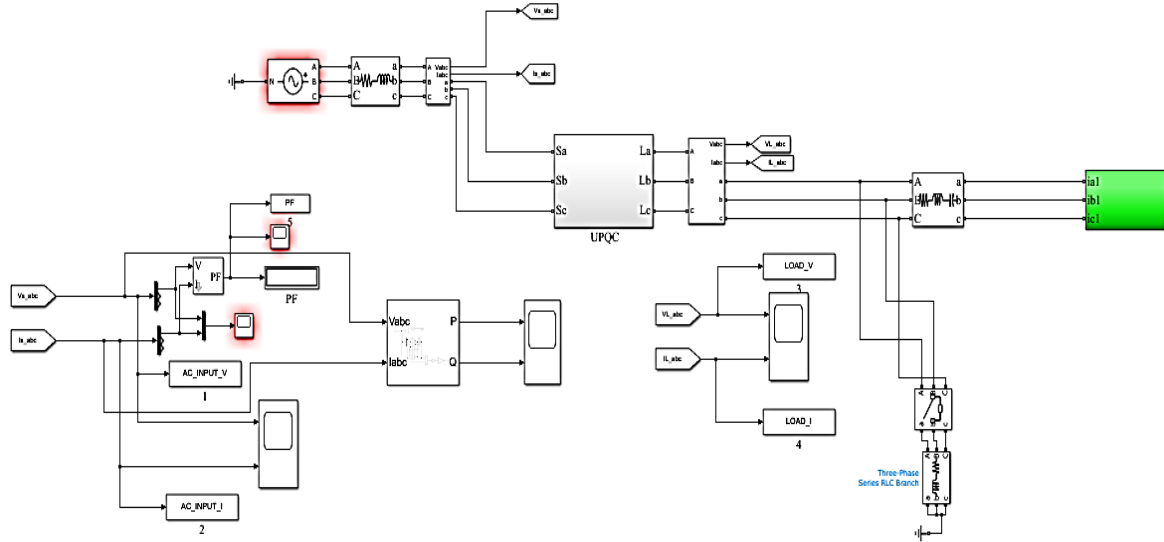


Figure 9. Simulation setup of the proposed work

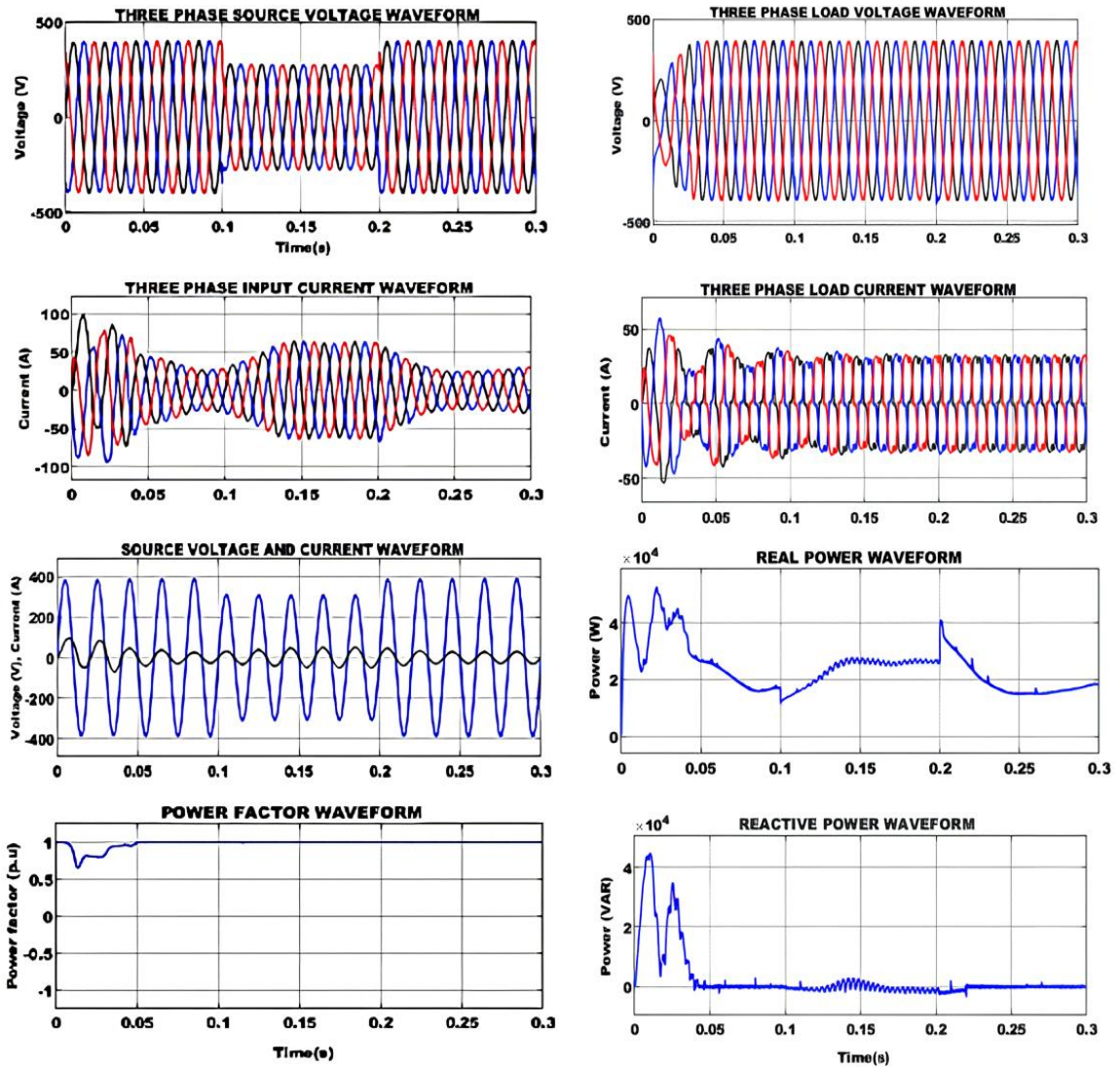


Figure 10. Case 1 simulation waveforms

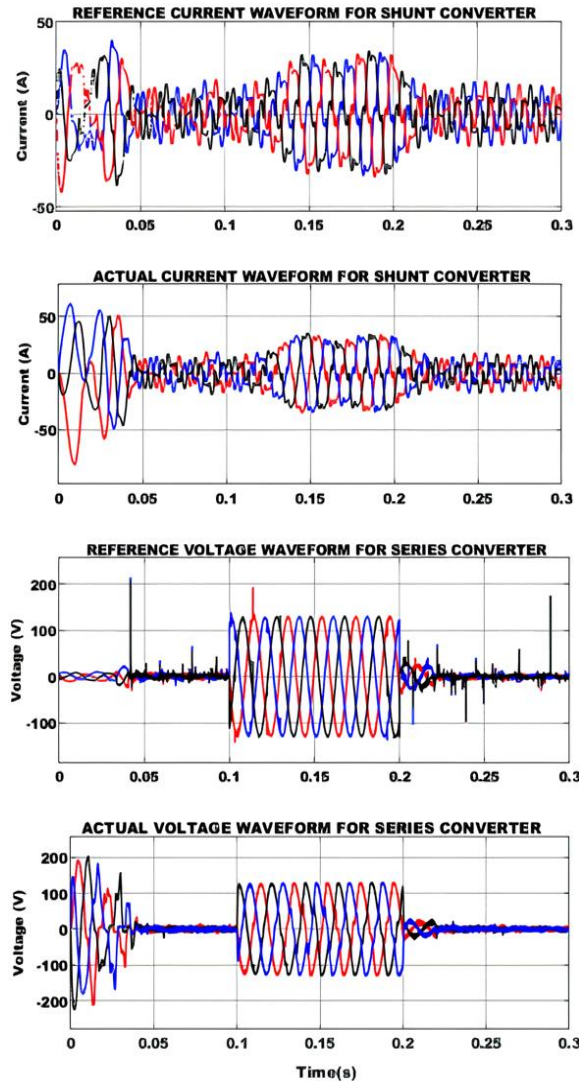


Figure 11. Case 1 compensator waveforms

Table 2. Specifications for simulation

Parameters	Values
Source Current	0-30 A
Source Voltage	330-470 V
Load Resistance	100 Ω
Load Inductance	10 mH

ii) Case 2: For step magnitude +0.3

The dynamic working of the proposed WECS fed UPFC is assessed under voltage swell in case 2. The source voltage is impacted by voltage swell of 0.3 p.u between 0.1 s to 0.2 s. Unlike case 1, a minimization of current magnitude is observed during voltage swell as seen in Figure 12. Variations are seen in source current in accordance to the voltage swell is better understood by considering the phase A of both these parameters as seen in Figure 12. Our proposed WECS fed UPFC is also capable of balancing voltage swell condition, since both the load voltage and load current waveforms are observed to be steady. A real and reactive power waveforms during voltage swell condition is also given in Figure 12.

The reference signals required for mitigating the voltage swell condition is obtained using DQ theory. The reference current is generated in the dq reference frame and is used to control the current of the proposed system. The series compensator generates the necessary voltage signal of opposite phase to compensate voltage swell as seen in Figure 13. The shunt converter would inject reactive power to maintain the load voltage at the reference level, while the series converter would inject voltage to mitigate the sag.

The DFIG output voltage waveform is given in Figure 14(a), it is square type waveform, which is not uniform in nature due to the variations in wind speed. This variable DFIG output is fed to the PWM rectifier and a stable output is generated with the assistance of CFLC as illustrated in Figure 14(b). The output waveform of the PWM rectifier in a DFIG system is a pulsating DC waveform with a ripple frequency equal to the switching frequency of the rectifier. The magnitude of the DC voltage is controlled by the amplitude of the AC output voltage of the DFIG, while the duty cycle of the rectifier switches is controlled by a PWM technique to produce the desired DC voltage level. Moreover, it is also noted that a stable DC voltage is maintained as seen in Figure 14(c).

Due to the effective compensation of PQ disturbances, the power factor is maintained as unity. Thereby a lower THD value of 2.55% is obtained using the proposed technique as indicated in Figure 15. The THD of the proposed UPFC is significantly reduced with the aid of the adopted control approach. The THD obtained with the CFLC is comparatively very less than THD values obtained using FLC and PI controllers as noted in Figure 16.

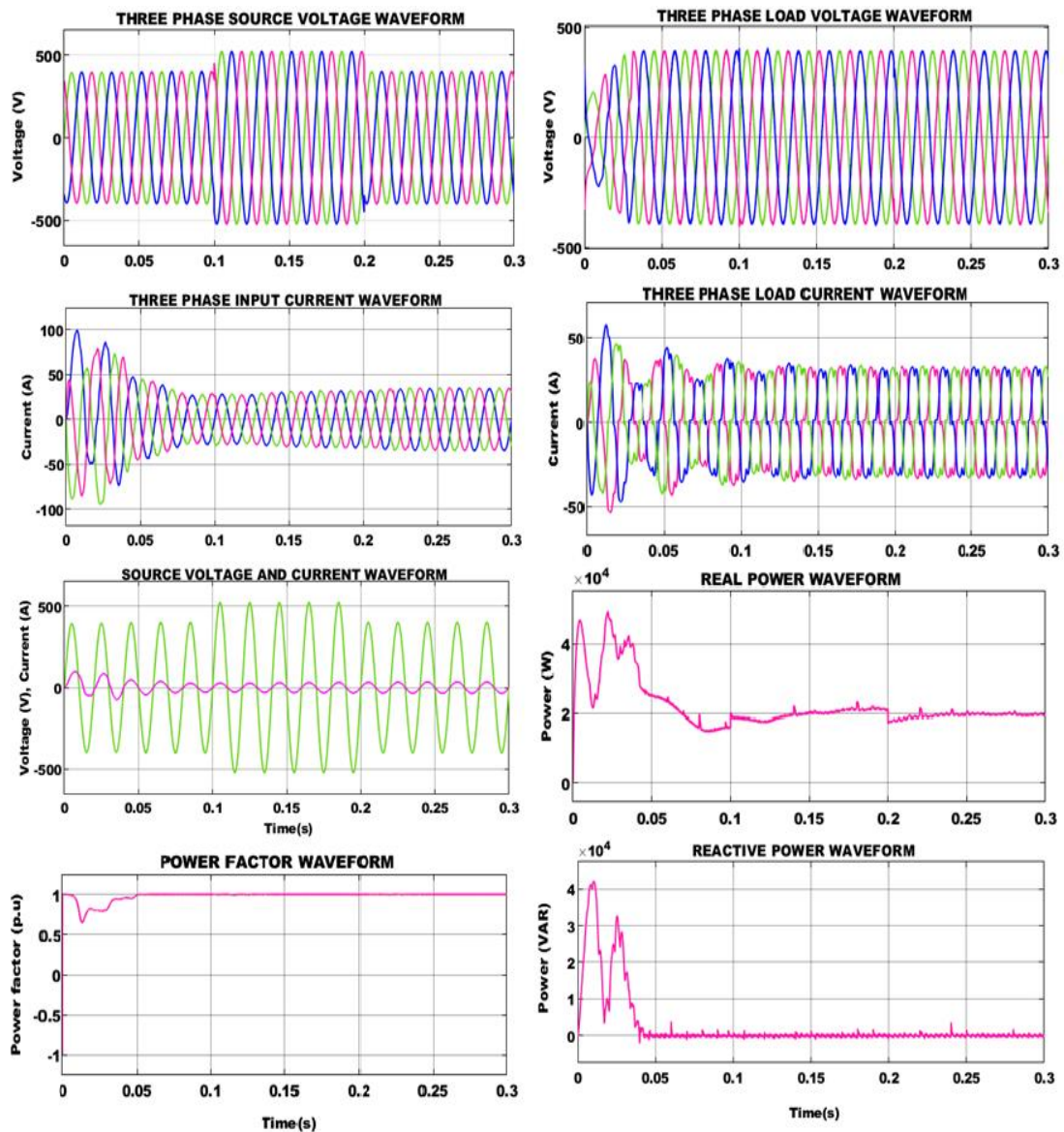


Figure 12. Case 2 simulation waveforms

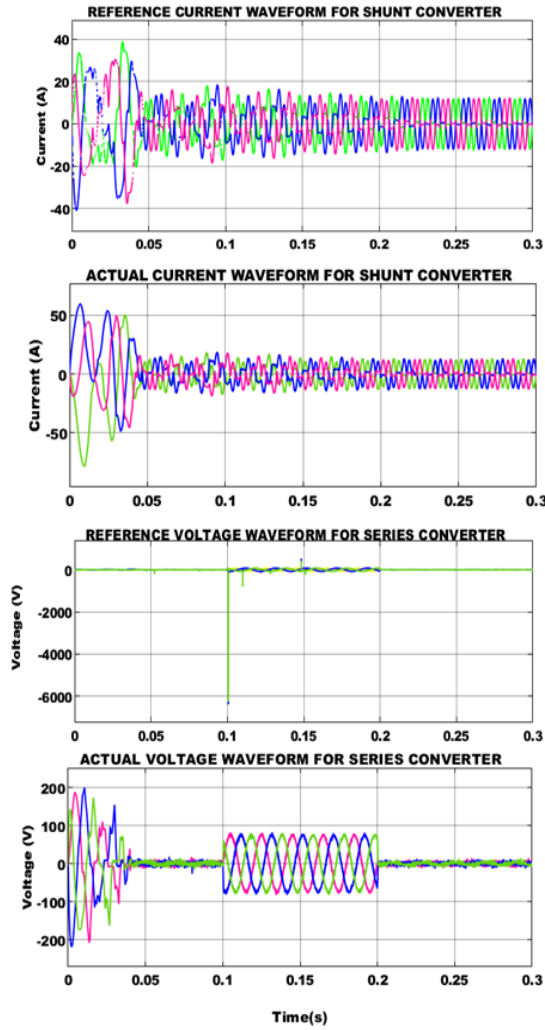


Figure 13. Case 2 compensator waveforms

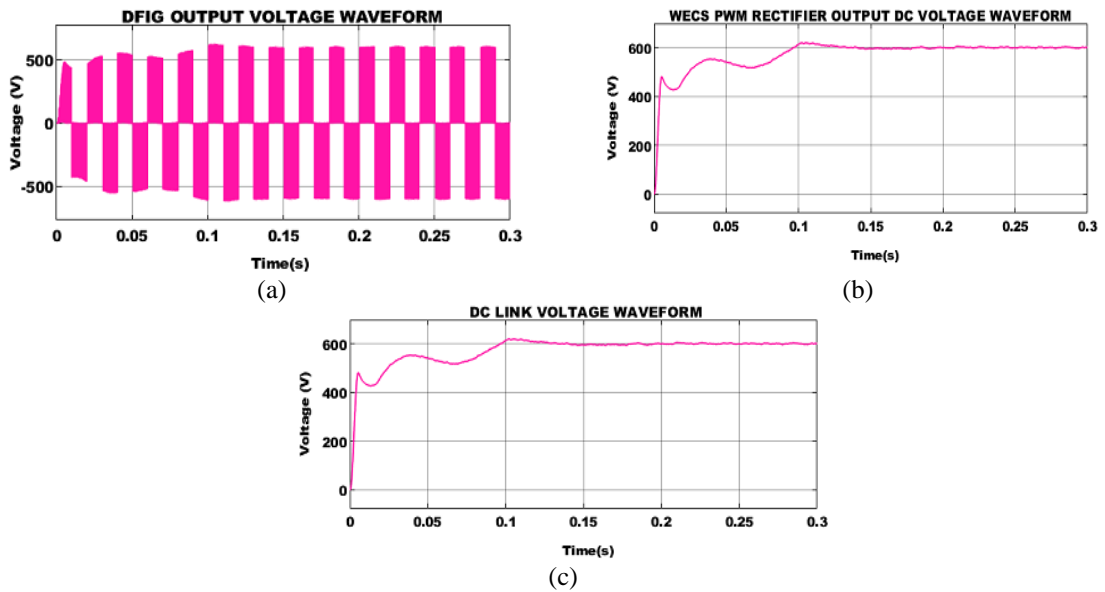


Figure 14. Temporal behavior of key voltage parameters in DFIG: (a) output voltage, (b) PWM rectifier output voltage, and (c) DC-link voltage

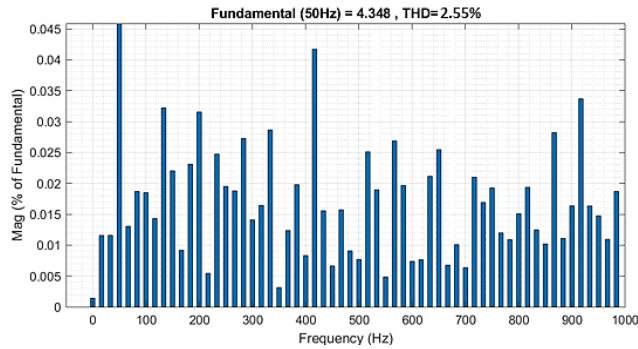


Figure 15. THD waveform

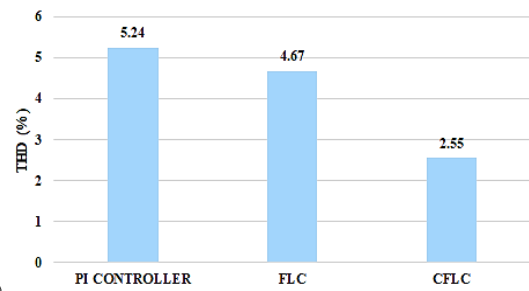


Figure 16. THD comparison

6. CONCLUSION

The modern-day power network is becoming increasingly complex due to the influx of several sustainable energy sources along with the increase in quantity of power electronic devices and nonlinear loads. This increase in complexity along with the deregulation of power sector has come at the cost of system instability due to increase in PQ issues. Hence, a WECS fed UPFC that provides the much needed stability to the power system along with facilitating a large-scale expansion of wind energy is proposed. The WECS output is made stable with the employment of CFLC, which offers faster error compensation. Moreover, in case of UPFC, the reference signals for the compensators are generated using DQ theory. DC-link voltage is maintained constant using CFLC. The simulation model for the proposed WECS fed UPFC with intelligent control approaches is developed in MATLAB and its capability in solving voltage sag and voltage swell condition is ascertained. The proposed approach is efficient in ensuring a PQ and a unity power factor is produced, according to the results. Consequently, the THD of the proposed work is also very low at a value of 2.55%, which further accredits to the significance of the proposed PQ enhancement technique.

REFERENCES

- [1] S. M. Suhail Hussain, F. Nadeem, M. A. Aftab, I. Ali, and T. S. Ustun, "The emerging energy internet: Architecture, benefits, challenges, and future prospects," *Electronics (Switzerland)*, vol. 8, no. 9, 2019, doi: 10.3390/electronics8091037.
- [2] M. Sadiq, J. P. Ou, K. D. Duong, L. Van, T. Q. Ngo, and T. X. Bui, "The influence of economic factors on the sustainable energy consumption: evidence from China," *Economic Research-Ekonomska Istrazivanja*, vol. 36, no. 1, pp. 1751–1773, 2023, doi: 10.1080/1331677X.2022.2093244.
- [3] R. M. Elavarasan *et al.*, "A Comprehensive Review on Renewable Energy Development, Challenges, and Policies of Leading Indian States with an International Perspective," *IEEE Access*, vol. 8, pp. 74432–74457, 2020, doi: 10.1109/ACCESS.2020.2988011.
- [4] R. Z. Butt *et al.*, "Techno-Economic and Environmental Impact Analysis of Large-Scale Wind Farms Integration in Weak Transmission Grid from Mid-Career Repowering Perspective," *Sustainability (Switzerland)*, vol. 14, no. 5, 2022, doi: 10.3390/su14052507.
- [5] A. Sengupta, D. K. Das, and B. Subudhi, "A delay-dependent dynamic wide area damping controller for renewable energy integrated power system resilient to communication failure," *CSEE Journal of Power and Energy Systems*, vol. 9, no. 2, pp. 577–588, 2022, doi: 10.17775/CSEEJPES.2022.02600.
- [6] P. Li, Y. Wang, C. Feng, and J. Lin, "Application of MMC-UPFC in the 500 kV power grid of Suzhou," *The Journal of Engineering*, vol. 2017, no. 13, pp. 2514–2518, 2017, doi: 10.1049/joe.2017.0780.
- [7] A. M. Shiddiq Yunus, A. Abu-Siada, M. I. Mosaad, H. Albalawi, M. Aljohani, and J. X. Jin, "Application of SMES Technology in Improving the Performance of a DFIG-WECS Connected to a Weak Grid," *IEEE Access*, vol. 9, pp. 124541–124548, 2021, doi: 10.1109/ACCESS.2021.3110995.
- [8] M. Ebeed, S. Kamel, J. Yu, and F. Jurado, "Development of UPFC operating constraints enforcement approach for power flow control," *IET Generation, Transmission and Distribution*, vol. 13, no. 20, pp. 4579–4591, 2019, doi: 10.1049/iet-gtd.2018.5609.
- [9] H. Samet, S. Ketabipour, M. Afrasiabi, S. Afrasiabi, and M. Mohammadi, "Deep learning forecaster-based controller for SVC: wind farm flicker mitigation," *IEEE Transactions on Industrial Informatics*, vol. 18, no. 10, pp. 7030–7037, 2022, doi: 10.1109/TII.2020.3025101.
- [10] M. N. H. Shazon, and H. M. Ahmed, "Modelling and utilisation of frequency responsive TCSC for enhancing the frequency response of a low inertia grid," *Energy Reports*, vol. 8, pp. 6945–6959, 2022, doi: 10.1016/j.egy.2022.05.101.
- [11] Y. Zhang, Y. Yang, X. Chen, and C. Gong, "Intelligent parameter design-based impedance optimization of STATCOM to mitigate resonance in wind farms," *IEEE Journal of Emerging and Selected Topics in Power Electronics*, vol. 9, no. 3, pp. 3201–3215, 2021, doi: 10.1109/JESTPE.2020.3020434.
- [12] Y. Li, Q. Zhou, S. Mu, T. Zhang, H. Li, and J. Wang, "A Sliding Mode SVPWM Method for a HTS Shunt Active Power Filter," *IEEE Transactions on Applied Superconductivity*, vol. 31, no. 8, 2021, doi: 10.1109/TASC.2021.3117746.
- [13] R. Mallajoshula and I. E. S. Naidu, "Novel MAF-Fuzzy Based IR-SRF Controller for DVR to Improve PQ Under Dynamic Weak Grid Conditions," *IETE Journal of Research*, 2022, doi: 10.1080/03772063.2021.2021821.
- [14] L. Wang *et al.*, "Damping of Subsynchronous Resonance in a Hybrid System with a Steam-Turbine Generator and an Offshore Wind Farm Using a Unified Power-Flow Controller," *IEEE Transactions on Industry Applications*, vol. 57, no. 1, pp. 110–120, 2021, doi: 10.1109/TIA.2020.3032934.
- [15] S. Rezaeian-Marjani, S. M. Jalalat, B. Tousi, S. Galvani, and V. Talavat, "A probabilistic approach for optimal operation of wind-integrated power systems including UPFC," *IET Renewable Power Generation*, vol. 17, no. 3, pp. 706–724, 2023, doi: 10.1049/rpg2.12627.

- [16] S. Ghaedi, S. Abazari, and G. Arab Markadeh, "Novel non-linear control of DFIG and UPFC for transient stability increment of power system," *IET Generation, Transmission and Distribution*, vol. 16, no. 19, pp. 3799–3813, 2022, doi: 10.1049/gtd2.12546.
- [17] N. K. Sakthivel and S. Sutha, "A novel algorithm of MGWO-based PI controller for a single-stage grid-connected flyback inverter with ZVS," *Automatika*, vol. 63, no. 1, pp. 64–77, 2022, doi: 10.1080/00051144.2021.2005288.
- [18] K. Sarita *et al.*, "Power Enhancement with Grid Stabilization of Renewable Energy-Based Generation System Using UPQC-FLC-EVA Technique," *IEEE Access*, vol. 8, pp. 207443–207464, 2020, doi: 10.1109/ACCESS.2020.3038313.
- [19] A. Kaymanesh, M. Babaie, A. Chandra, and K. Al-Haddad, "PEC Inverter for Intelligent Electric Spring Applications Using ANN-Based Controller," *IEEE Journal of Emerging and Selected Topics in Industrial Electronics*, vol. 3, no. 3, pp. 704–714, 2021, doi: 10.1109/jestie.2021.3095018.
- [20] M. I. Mosaad, A. Alenany, and A. Abu-Siada, "Enhancing the performance of wind energy conversion systems using unified power flow controller," *IET Generation, Transmission and Distribution*, vol. 14, no. 10, pp. 1922–1929, 2020, doi: 10.1049/iet-gtd.2019.1112.
- [21] S. Vig and B. S. Surjan, "Optimal power dispatch of WECS and UPFC with ACO and ANFIS algorithms," *International Journal on Electrical Engineering and Informatics*, vol. 10, no. 1, pp. 14–36, 2018, doi: 10.15676/ijeii.2018.10.1.2.
- [22] P. R. Sankarganesh, B. Ashok Kumar, and M. E. Tech, "Mitigation of Harmonics and Power Quality Improvement for Grid-Connected Wind Energy System using Unified Power Flow Controller Based on Spontaneous Energy Optimization Algorithm," *International Journal of Engineering Inventions*, vol. 8, no. 1, pp. 92–101, 2019, [Online]. Available: www.ijeijournal.com
- [23] S. R. Abbas *et al.*, "Impact analysis of large-scale wind farms integration in weak transmission grid from technical perspectives-," *Energies*, vol. 13, no. 20, p. 5513, Oct. 2020, doi: 10.3390/en13205513.
- [24] O. P. Mahela, B. Khan, H. H. Alhelou, and P. Siano, "Power Quality Assessment and Event Detection in Distribution Network with Wind Energy Penetration Using Stockwell Transform and Fuzzy Clustering," *IEEE Transactions on Industrial Informatics*, vol. 16, no. 11, pp. 6922–6932, 2020, doi: 10.1109/TII.2020.2971709.
- [25] M. Maleki Rizi, S. Abazari, and N. Mahdian, "Dynamic Stability Improvement of Power System with Simultaneous and Coordinated Control of DFIG and UPFC using LMI," *International Journal of Industrial Electronics Control and Optimization*, vol. 4, no. 3, pp. 341–353, 2021.

BIOGRAPHIES OF AUTHORS



Polishetty Vinay Kumar    received his B. Tech Degree in the year 2010 from JNTU Hyderabad. He received M. Tech (Power System) from JNTU Hyderabad in the year 2014 and presently he is pursuing Ph. D from Annamalai University Chidambaram. His research interest includes power systems, power system stability and reliability, machines, power electronics and drives. He can be contacted at email: vinaykumarpolishetty@gmail.com.



Balamurugan Ganapathi    obtained his Bachelor's degree from Annamalai University, Chidambaram in 1993, Master's degree from Annamalai University in 1995 and Doctoral degree in Electrical Engineering from Annamalai University in 2012. He is currently serving as Professor in the Department of Electrical Engineering at Annamalai University, Chidambaram, India. His areas of interest include power system economics, voltage stability, restricted power system. He can be contacted at email: abi_senthil10@rediffmail.com.



Kartigeyan Jayaraman    obtained his Bachelor's degree in Electrical and Electronics Engineering from Madras University in 2004, Master's degree in Electrical Drives and Control from Pondicherry University in 2007 and Doctoral degree in Electrical Engineering from Annamalai University in 2017. He is currently serving as Associate Professor in the Department of Electrical and Electronics Engineering and Dean Student Affairs at J.B. Institute of Engineering and Technology, Hyderabad, India. He has a number of publications in National and International journals to his credit. His areas of interest include core loss modelling, magnetic materials, design and control of switched reluctance and ac machines. He can be contacted at email: j.kartigeyan@gmail.com.